

Observation of Barrier Inhomogeneity in Pt/*a*-plane n-type GaN Schottky Contacts

Soo-Hyon PHARK

Max-Planck-Institut für Mikrostrukturphysik, Weinberg 2, D-06120 Halle, Germany

Hogyoung KIM*

College of Humanities and Sciences, Hanbat National University, Daejeon 305-719, Korea

Keun-Man SONG

Korea Advanced Nano Fab Center, Suwon 443-270, Korea

Dong-Wook KIM

*Department of Physics, Department of Chemistry and Nano Science,
Ewha Womans University, Seoul 120-720, Korea*

(Received 30 July 2010)

We carried out microscale and nanoscale investigations of the electrical properties of Pt/*a*-plane n-type GaN Schottky contacts. Using the thermionic emission (TE) model, we observed that both the barrier heights and ideality factors varied from diode to diode with a linear relationship between them, indicating a spatial fluctuation of barrier height. The thermionic field emission (TFE) model produced a better fit to the experimental current-voltage data than the TE model, which suggested that tunneling, probably due to the presence of a large number of surface defects, played an important role in the Pt/*a*-plane n-type GaN Schottky contacts. A two-dimensional current map of the Schottky junctions using conductive atomic force microscopy revealed an inhomogeneous spatial current distribution, which confirmed the existence of an inhomogeneous barrier in the Schottky diodes.

PACS numbers: 85.30.De, 81.05.Ea

Keywords: *a*-plane GaN, Inhomogeneous barrier, Current map

DOI: 10.3938/jkps.58.1356

I. INTRODUCTION

III-nitrides are very attractive materials for optoelectronic devices, such as light-emitting diodes (LEDs) and blue/ultraviolet lasers, because of their direct and wide band-gap [1]. However, optoelectronic devices based on *c*-plane (0001) heterostructures are significantly affected by spontaneous and piezoelectric polarizations due to the quantum-confined Stark effect [2]. Polarization-induced electric fields can spatially separate electrons and holes within quantum wells, reducing the luminescence efficiency and shifting the light emission to longer wavelengths than in polarization-free structures [3]. The growth of GaN films in directions perpendicular to the *c*-axis has been researched as a means of eliminating these polarization-related effects in nitride-based optoelectronic devices [4]. Despite the progress in GaN-

based devices, the device performance is limited by the presence of extended defects due to the thermal, lattice, and symmetry mismatches with the sapphire substrates, acting as nonradiative recombination centers and negatively-charged scattering centers [5,6].

Characterization of the electrical properties of metal-GaN contacts has the potential to elucidate the nature of the transport and the role of defects in determining the contact characteristics, which will contribute to realizing high-performance GaN-based devices. Sawada *et al.* [7] used potential pinch-off due to small patches of crystal defects, such as dislocations and micropipes, to explain the electron transport in n-type GaN (n-GaN). The electrical properties of Pt contacts to n-GaN have been investigated in terms of the inhomogeneous barriers and were correlated to a nanoscale electrical characterization of the barrier [8]. The transport properties of *a*-plane n-GaN contacts, however, have rarely been studied [9, 10]. In this work, Pt Schottky contacts were fabricated

*E-mail: hoyoungkim@gmail.com; Fax: +82-42-821-1599

on *a*-plane n-GaN, and the properties were investigated on both a micro and nanoscale.

II. EXPERIMENT

Si-doped nonpolar *a*-plane (11 $\bar{2}$ 0) n-GaN thin films grown on *r*-plane (1 $\bar{1}$ 02) sapphire substrates by using metalorganic chemical vapor deposition (MOCVD) were used in this study. The electron concentration and mobility determined by Hall-effect measurements were $1 - 2 \times 10^{18} \text{ cm}^{-3}$ and $60 - 80 \text{ cm}^2/\text{V}\cdot\text{s}$, respectively. Planar Pt Schottky diodes were fabricated using standard photolithography. The fabrication procedure of the Schottky diodes has been described in detail elsewhere [11]. Microscale current-voltage (*I-V*) measurements (denoted as “microscale *I-V*”) were performed using a semiconductor parameter analyzer (HP 4156B), and nanoscale *I-V* measurements (denoted as “nanoscale *I-V*”) were carried out using a conductive atomic force microscopy (C-AFM) system (Nanofocus Albatross II) with nitrogen-doped diamond-coated Si tips (NT-MDT Co.). An enhancement in the lateral resolution of the C-AFM could be expected by introducing an ultrathin ($\sim 3 \text{ nm}$) Pt metal layer between the metallic tip and the sample surface because it may enable ballistic transport perpendicular to itself on one hand and decrease the in-plane transport due to the high lateral resistance on the other hand [12].

III. RESULTS AND DISCUSSION

Figure 1(a) shows the microscale *I-V* characteristics measured from several Schottky diodes. With the assumption of thermionic emission (TE) being the major forward current contribution, the diode current can be determined as [13]

$$I = I_0 [\exp(q(V - IR_S)/nk_B T) - 1], \quad (1)$$

$$I_0 = AA^{**}T^2 \exp(-q\phi_B/k_B T), \quad (2)$$

where A is the device area, A^{**} is the effective Richardson constant ($26.4 \text{ A/cm}^2\text{K}^2$ for n-GaN), ϕ_B is the effective barrier height and V is the applied voltage. The barrier height and the ideality factor were determined to be $0.47 (\pm 0.03) \text{ eV}$ and $1.60 (\pm 0.09)$, respectively. As shown in Fig. 1(b), both the barrier heights and the ideality factors varied from diode to diode with a linear relationship between barrier height and ideality factor, indicating the presence of a lateral inhomogeneity in the Schottky barrier. In our previous work, we found the barrier inhomogeneity of the Pt/*a*-plane n-GaN contact by using current-voltage-temperature (*I-V-T*) measurements [11]. In order to explain the observed barrier inhomogeneity, we utilized a modified Richardson plot, which adopts a lateral variation of the barrier height with a Gaussian distribution over the Schottky contact area

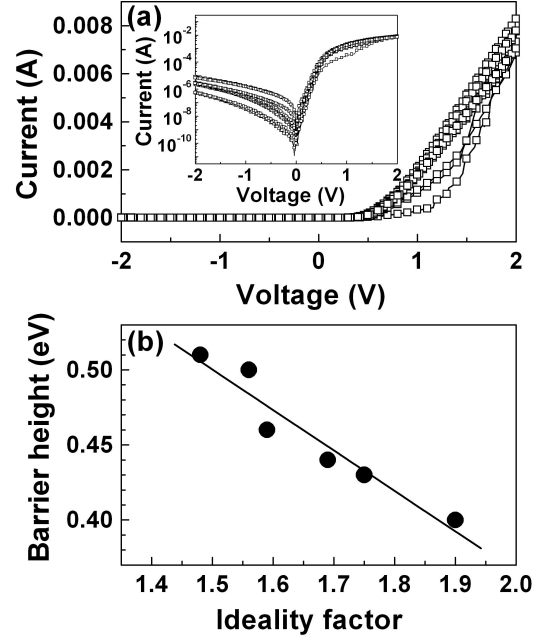


Fig. 1. (a) *I-V* characteristics of Pt Schottky contacts to *a*-plane n-GaN measured at room temperature and (b) barrier height versus ideality factor plot. The inset in (a) shows the $\log(I)$ versus V plot, and the line in (b) is a linear fit to the data.

[14]. The determined Richardson constant was $2.26 \times 10^5 \text{ A/cm}^2\text{K}^2$, which is much larger than the theoretical value of $26.4 \text{ A/cm}^2\text{K}^2$. This indicates that the TE model, even including the inhomogeneous barrier height effects, cannot explain the transport characteristics of the Pt Schottky contacts to *a*-plane n-GaN. The similarity between barrier heights from the thermionic field emission (TFE) model and the flat-band condition suggest that the TFE model is more appropriate to explain the current transport in Pt/*a*-plane n-GaN Schottky contacts.

In order to verify such results further, we calculated the *I-V* characteristics by using both the TE and the TFE models and compared these to the experimental *I-V* characteristics. Here, the forward current I_F and the reverse current I_R using the TFE model are given by [15]

$$\begin{aligned} I_F &= I_{F0} \exp\left(\frac{qV}{E_{00} \coth(E_{00}/k_B T)}\right) \\ &= I_{F0} \exp\left(\frac{qV}{E_0}\right), \end{aligned} \quad (3)$$

$$\begin{aligned} I_{F0} &= A \frac{A^{**}T \sqrt{\pi E_{00} q (\phi_B - V - \xi)}}{k \cosh(E_{00}/k_B T)} \\ &\times \exp\left[-\frac{q\xi}{k_B T} - \frac{q(\phi_B - \xi)}{E_{00} \coth(E_{00}/k_B T)}\right], \end{aligned} \quad (4)$$

$$I_R = I_{R0} \exp\left(\frac{qV}{k_B T} - \frac{qV}{E_{00} \coth(E_{00}/k_B T)}\right), \quad (5)$$

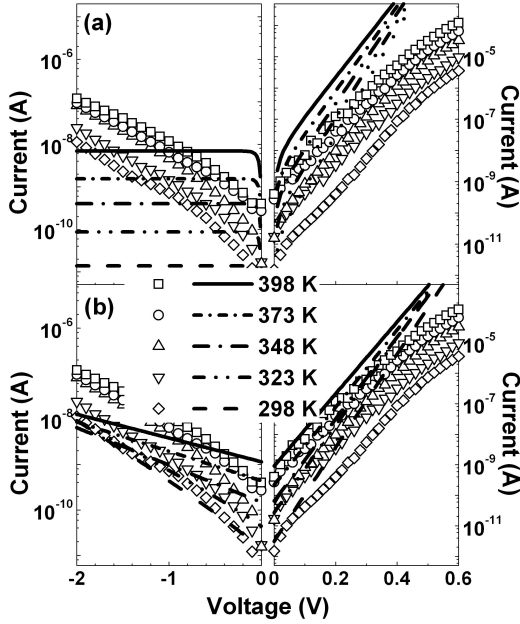


Fig. 2. Experimental I - V characteristics (open symbols) and I - V characteristics (lines) calculated using the (a) TE model and (b) the TFE model.

$$I_{RO} = A \frac{A^{**} T \sqrt{\pi E_{00}}}{k} \sqrt{q(V - \xi) + \frac{q\phi_V}{\coth^2(E_{00}/k_B T)}} \times \exp \left[-\frac{q\phi_B}{E_{00} \coth(E_{00}/k_B T)} \right], \quad (6)$$

where $E_{00} = qh/4\pi (N_D/m^* \epsilon)^{1/2}$ is the characteristic energy related to the tunneling probability and $\xi = k_B T/q \ln(N_C/N_D)$ is the energy difference between E_C and E_F , with N_C being the effective density of states in the conduction band and N_D the carrier concentration. The I - V curves calculated using the TE model are indicated by lines in Fig. 2(a). Large deviations from the TE behavior are clearly seen in both the forward and the reverse currents. Assuming $E_{00} = 12.6$ meV obtained from the carrier concentration of $N_D = 1 \times 10^{18} \text{ cm}^{-3}$, the I - V characteristics calculated by using the TFE model with Eqs. (3) - (6) are shown by lines in Fig. 2(b). The TFE model shows a better fit to the experimental I - V data than the TE model, although there is still some discrepancy between the experimental and the calculated I - V data. Therefore, we can conclude that tunneling, which may occur due to the large number of surface defects, plays an important role in the Pt/ a -plane n-GaN contacts [16].

Figure 3(a) shows the nanoscale I - V characteristics obtained from the C-AFM measurements. The I - V data show the rectifying behavior, indicating nanoscale Schottky contact formation of the Pt film on a -plane n-GaN. When observing the reverse-biased current profiles in Fig. 3(b), both the micro and nanoscale transport characteristics show similar behaviors. Thus, we can specu-

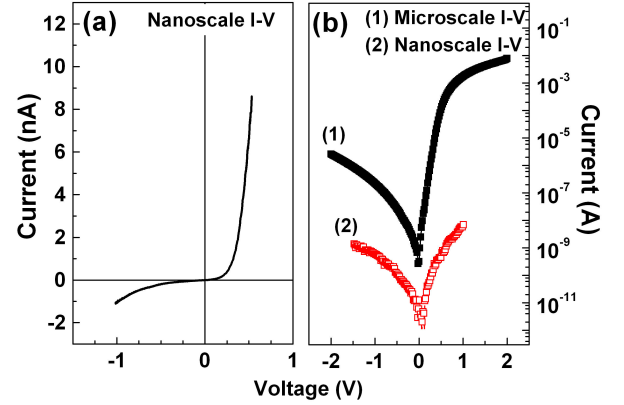


Fig. 3. (Color online) (a) Linear nanoscale I - V characteristic and (b) semi-logarithmic microscale and nanoscale I - V characteristics.

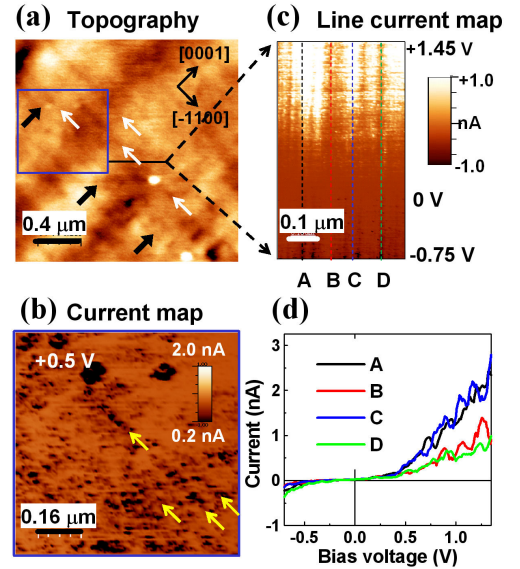


Fig. 4. (Color online) (a) AFM topographic image, $2 \times 2 \mu\text{m}^2$, obtained for the Pt/ a -plane n-GaN device, (b) C-AFM current map of the region, $0.8 \times 0.8 \mu\text{m}^2$, boxed by the blue square in (a), (c) line current map along the black line in (a), and (d) current profiles along the lines corresponding to the four points indicated by A, B, C, and D in (c).

late that both the micro and nanoscale I - V data have the same current density profile when considering different junction areas, which implies that there is negligible leakage current around the periphery of the junction area and the measured I - V characteristics can be regarded as current values representing bulk Schottky barrier currents [17]. The barrier height and the ideality factor for the nanoscale I - V data were calculated to be $0.35 (\pm 0.02)$ eV and $2.89 (\pm 0.12)$, respectively. The enhanced tunneling current due to the reduced depletion width in the case of a nanoscale Schottky contact might cause the higher ideality factor and the lower barrier height [18].

Figure 4(a) shows an AFM topographic image of the Pt/*a*-plane n-GaN device. We found groovy structural modulations running along the [0001] direction, as denoted by black thick arrows. The origin of these modulations was attributed to the different adatom incorporation rate between the [0001] and the $[\bar{1}100]$ directions [19]. Other characteristic features are the line patterns along the $[\bar{1}100]$ directions, as indicated by white arrows, which have heights slightly lower than that of the background surface. Figure 4(b) shows the C-AFM current map obtained from the boxed region in Fig. 4 (a) simultaneously with the topographic image [Fig. 4(a)]. It shows the inhomogeneous current distribution throughout the region. A more impressive character is the narrow line shape distribution of the rather low current regions arranged along the $[\bar{1}100]$ direction, as denoted by the yellow arrows.

To investigate the relevance of the local junction characteristics to the topographic variation, we obtained a set of current profiles with respect to the position and the bias voltage (V_B) along a single topographic line, a so-called ‘line current map’. We repeatedly scanned the black line in Fig. 4(a) while varying V_B from -0.75 to 1.45 V and obtained the line current map as shown in Fig. 4(c). One can note that the current flow as a function of V_B highly depends on the position. The current profiles along the four dashed lines in Fig. 4(c), in which an individual curve represents the I - V characteristics at each selected position, are shown in Fig. 4(d). Although it is hard to extract common junction characteristics due to the noisy curve shapes, one can distinguish clearly the dependence of the current level on the measured position. This is consistent with the existence of low-current regions in the current map [Fig. 4(b)]. Also, with the fact that the directions of such low-current regions were arranged along the $[\bar{1}100]$ direction, the observations in Figs. 4(c) and (d) suggest a direct relation between the spatial inhomogeneity in the local I - V characteristics and the structural line patterns found in Fig. 4(a).

A C-AFM and near-field optical microscopy (NSOM) study on the properties of *a*-plane GaN films grown via epitaxial lateral overgrowth (ELO) by using MOCVD demonstrated the correlation between the presence of surface pits and leakage sites [19]. From the structural similarities to the line defects along the $[\bar{1}100]$ direction of *a*-plane AlN and GaN [20], which are supposed to be the protruded edges of the stacking faults in the *c*-plane, the line-type structures in Fig. 4(a) seem to stem from the stacking faults lying in the (0001) plane. Comparative studies of the topography and the current distribution of Pt/*a*-plane GaN show that such defects may cause a reduction in the tip-sample nanojunction current due to rather the large barrier height [21]. Resultantly, the observations in Figs. 4 suggest that the surface microstructures may modify the local junction characteristics in Pt/*a*-plane n-GaN Schottky contacts, implying an inhomogeneous barrier. Therefore, both the nonuniform dis-

tribution of surface pits and surface microstructures may lead to an inhomogeneous barrier height with the dominant transport mechanism being TFE. Further structural analyses with higher spatial resolution are needed to clarify the origin of the TFE transport across the Schottky junction in the Pt/*a*-plane n-GaN.

IV. CONCLUSION

In conclusion, we investigated the electrical properties for Pt/*a*-plane n-type GaN Schottky contacts. Using the thermionic emission (TE) model, it was observed that both the barrier heights and ideality factors varied from diode to diode with a linear relationship between them, indicating the spatial fluctuation of barrier height. Two-dimensional current maps of the Schottky junctions using C-AFM revealed an inhomogeneous spatial current distribution, which well supported our analyses including the inhomogeneous barrier feature.

ACKNOWLEDGMENTS

This work was supported by Ministry of Education, Science and Technology (MEST) and Daegu Gyeongbuk Institute of Science and Technology (DGIST) (10-BD-0101, Convergence Technology with New Renewable Energy and Intelligent Robot).

REFERENCES

- [1] S. Nakamura and G. Fasol, *The Blue Laser Diode* (Springer, Berlin, 1997).
- [2] F. Bernnardini, V. Fiorentini and D. Vanderbilt, Phys. Rev. B **56**, R10024 (1997).
- [3] E. T. Yu, G. J. Sullivan, P. M. Asbeck, C. D. Wang, D. Qiao and S. S. Lau, Appl. Phys. Lett. **71**, 2794 (1997).
- [4] M. D. Craven, S. H. Lim, F. Wu, J. S. Speck and S. P. DenBaars. Appl. Phys. Lett. **81**, 469 (2002).
- [5] J. W. P. Hsu, D. V. Lang, S. Richter, R. N. Kleiman, A. M. Sergent and R. J. Molnar, Appl. Phys. Lett. **77**, 2873 (2000).
- [6] N. G. Weimann, L. F. Eastman, D. Doppalapudi, H. M. Ng and T. D. Moustakas, J. Appl. Phys. **83**, 3656 (1998).
- [7] T. Sawada, N. Kimura, K. Imai, K. Suzuki and K. Tanahashi, J. Vac. Sci. Technol., B **22**, 2051 (2004).
- [8] F. Iucolano, F. Rocafort, F. Giannazzo and V. Raineri, J. Appl. Phys. **102**, 113701 (2007).
- [9] V. Adivarahan, C. Chen, J. Yang, M. Gaevski, M. Shatalov, G. Simin and M. Asif Khan, Jpn. J. Appl. Phys. **42**, L1136 (2003).
- [10] H. Kim, S. N. Lee, Y. Park, J. S. Kwak and T. Y. Seong, Appl. Phys. Lett. **93**, 032105 (2008).
- [11] S. H. Phark, H. Kim, K. M. Song, P. G. Kang, H. S. Shin and D. W. Kim, J. Phys. D: Appl. Phys. **43**, 165102 (2010).

- [12] F. Giannazzo, F. Roccaforte, V. Raineri and S. F. Liotta, *Europhys. Lett.* **74**, 686 (2006).
- [13] S. M. Sze, *Physics of Semiconductor Devices* (Wiley, New York, 1981).
- [14] J. H. Werner and H. H. Gutter, *J. Appl. Phys.* **69**, 1522 (1991).
- [15] F. A. Padovani and R. Stratton, *Solid-State Electron.* **9**, 695 (1966).
- [16] T. Hashizume, J. Kotani and H. Hasegawa, *Appl. Phys. Lett.* **84**, 4884 (2004).
- [17] J. Kotani, T. Hashizume and H. Hasegawa, *J. Vac. Sci. Technol., B* **22**, 2179 (2004).
- [18] G. D. J. Smit, R. Rogge and T. M. Klapwijk, *Appl. Phys. Lett.* **8**, 3852 (2002).
- [19] J. C. Moore, V. Kasliwal, A. A. Baski, X. Ni, Ü. Özgür and H. Morkoç, *Appl. Phys. Lett.* **90**, 011913 (2007).
- [20] H. Wang, C. Chen, Z. Gong, J. Zhang, M. Gaevski, M. Su, J. Yang and M. A. Khan, *Appl. Phys. Lett.* **84**, 499 (2004).
- [21] S. H. Phark, H. Kim, K. M. Song, P. G. Kang, H. S. Shin and D. W. Kim, *J. Nanosci. Nanotechnol.* **11**, 1413 (2011).